JOURNAL OF CATALYSIS 81, 147–167 (1983)

Metal–Support Interactions between Iron and Titania for Catalysts Prepared by Thermal Decomposition of Iron Pentacarbonyl and by Impregnation

JEANNETTE SANTOS, J. PHILLIPS,[1] AND J. A. DUMESIC[2]

Department of Chemical Engineering, University of Wisconsin–Madison, Madison, Wisconsin 53706

Received October 11, 1982; revised December 13, 1982

Metallic iron particles supported on titania were prepared by aqueous incipient wetness impregnation, nonaqueous impregnation, and thermal decomposition of iron pentacarbonyl. For iron loadings between 1 and 5 wt%, only the last technique produced metallic iron particles smaller than 10 nm, as judged by X-ray line-broadening and CO chemisorption measurements. During the decomposition of iron pentacarbonyl at 380 K, Mössbauer spectroscopy showed that Fe^{2+} and zero-valent iron (e.g., subcarbonyl species) were formed on titania, presumably due to the interaction of iron carbonyl with hydroxyl groups on the support surface; however, these iron species were reduced to metallic iron particles in hydrogen at ca. 700 K. The ammonia synthesis apparent activation energy, E_A, and ammonia partial pressure dependence, m, for all Fe/TiO_2 catalysts reduced at ca. 700 K were similar to those values for metallic iron supported on silica or magnesia. Upon increasing the reduction temperature to ca. 800 K, the values of E_A and m increased for Fe/TiO_2 catalysts with iron particles are large as 20 nm. Room temperature Mössbauer spectra of the Fe/TiO_2 catalysts after reduction at either 700 or 800 K indicated that the majority or the iron was present as α-Fe, with Mössbauer parameters essentially identical to bulk metallic iron. Accordingly, the metal–support interaction between iron and titania, which is initiated by reduction at 800 K and is responsible for the changes in ammonia synthesis kinetics, is due to titanium species at the surface of the metallic iron particles. This interaction, which also suppresses CO chemisorption, can be partially destroyed by exposure of the sample to air at room temperature. Possible modes of transport of titanium species during catalyst preparation, reduction, and oxidation are discussed.

INTRODUCTION

A number of studies have provided evidence for the existence of "strong metal–support interactions (SMSI)" between Group VIII metals and titania. Most of the pioneering work was done by Tauster *et al.* (*1, 2*) and Baker *et al.* (*3, 4*), and much of the more recent work in this area is contained in Refs. *5–12*, the papers quoted therein, and a recent symposium focusing on metal–support interactions (*13*). This has involved work using hydrogen and carbon monoxide chemisorption (*1, 2*), electron microscopy (*3, 4*), photoelectron spectroscopy (*8–10*), and catalytic measurements (*6, 7*). It is clear from these studies that reduction of titania-supported catalysts at high temperature (e.g., 770 K) causes a suppression of hydrogen and carbon monoxide chemisorption on the metal at room temperature. In addition, this may be accompanied by a change in the catalytic activity and selectivity of the metal (e.g., for hydrogenation and hydrogenolysis reactions), a change in the morphology of the metal particles (e.g., formation of pillbox or raft-like particles), and a slight shift in the binding energy of the metallic electrons (e.g., ±0.5 eV). What is unclear at present, however, is the origin of the metal–support interactions which are initiated by reduction at high temperatures. Perhaps the most widely accepted belief has been that strong metal–support interactions are related to

[1] Present address: Department of Chemical Engineering, Pennsylvania State University, University Park, Penn. 16802.

[2] To whom correspondence should be addressed.

0021-9517/83 $3.00

electron transfer between the metal and reduced forms of titania (TiO_{2-x}) (e.g., *5, 11, 12*).

The present study was undertaken to probe the nature of metal–support interactions between iron and titania. A previous series of papers (*10, 14–16*) involving the physical characterization of metallic iron particles supported on thin films of titania indicated that "normal" metallic iron (i.e., three-dimensional particles of α-Fe) can be formed upon hydrogen treatment at temperatures near 700 K, while an interaction between iron and titania is initiated when the reduction temperature is raised to ca. 770 K. In addition, the reduction temperature should not exceed 870 K, otherwise iron diffuses into the titania support and becomes unavailable for catalytic reactions. With these results in mind, the present study involves the use of Mössbauer spectroscopy, CO chemisorption, and ammonia synthesis reaction kinetics to characterize the physical, chemisorptive, and catalytic properties of Fe/TiO_2 catalysts prepared by different methods and reduced at temperatures between ca. 700 and 800 K. The most highly dispersed metallic iron particles were prepared by the thermal decomposition of iron pentacarbonyl, and emphasis is placed on the study of the preparation and characterization of these catalysts.

EXPERIMENTAL

Catalyst preparation. Incipient wetness impregnation of titania (Degussa P-25; Cabot Corp. Cab-O-Ti) was carried out using a saturated aqueous solution of ferric nitrate (Baker). The volume of solution used in the impregnations was 0.25 ml/g of titania. To obtain the desired wt% loading of iron (e.g., 5%), a number of impregnations were performed. After each impregnation, the catalyst was dried from 6 to 16 h in air at ca. 390 K. Sample preparation via incipient wetness impregnation with an acid solution was done in identical fashion, except for the utilization of a 1 *M* HNO_3 solution instead of water. Nonaqueous impregnation of titania was performed using an acetone solution (0.5 wt% water content) of ferric nitrate, $Fe(NO_3)_3 \cdot 9H_2O$ (ca. 5×10^{-3} *M*). Extented contact (e.g., 24 h) with occasional stirring was needed for the iron to be completely adsorbed on titania. During this process, the color of titania changed from white to bright yellow. The solution was centrifuged, the acetone was decanted, and the remaining solid was dried in air at ca. 390 K for 12 h.

Iron pentacarbonyl decomposition on titania was carried out using two glass apparatuses described elsewhere (*17, 18*). In short, liquid $Fe(CO)_5$ (Apache Chemical) was stored in a glass bulb connected to the first glass system, and another glass bulb, subsequently denoted as the transfer bulb, was filled with gaseous $Fe(CO)_5$ in the following manner. The transfer bulb and the main manifold were evacuated to ca. 10^{-1} Pa for about 1 h. Then the system was isolated from the rotary pump, the bulb with the liquid iron carbonyl was opened, and gaseous $Fe(CO)_5$ was allowed to equilibrate throughout the system. This procedure allowed a transfer bulb of known volume to be filled with $Fe(CO)_5$ at a known pressure (ca. 3.2 kPa, measured using a mercury manometer), and this bulb could be carried to other apparatuses where $Fe(CO)_5$ decomposition on titania could be performed.

A second glass apparatus was used to decompose $Fe(CO)_5$ on titania. The system was also used for CO chemisorption measurements and BET surface area determinations. For this purpose, the apparatus was equipped with a Texas Instruments precision pressure gage (Model 145). The transfer bulb containing gaseous iron carbonyl and a glass cell containing titania were both connected to the main manifold of this apparatus. After evacuation of the manifold and the cell, gaseous iron pentacarbonyl was expanded into the cell containing the titania, and $Fe(CO)_5$ decomposition was carried out for at least 12 h at 380 K in this static system. After decomposi-

tion of $Fe(CO)_5$, the samples were cooled to room temperature and evacuated, followed by reduction at 673 K for ca. 16 h and at 713 K for 1 h in hydrogen or ammonia synthesis gas ($H_2 : N_2 = 3 : 1$). The hydrogen (Chemetron, 99.8%) and the 3 : 1 $H_2 : N_2$ synthesis gas mixture (Matheson, prepurified, certified standard) were purified by flowing through a Deoxo gas purifier (Engelhard Industries), followed by a packed bed of 13× molecular sieves (Davison, 4–8 mesh) immersed in liquid nitrogen. After reduction, the catalyst was cooled in the reducing environment and the gas atmosphere was switched to nitrogen for ca. 0.10 h. Finally, the catalyst was exposed to air and used in Mössbauer spectroscopy or ammonia synthesis kinetics studies. Iron loadings on titania were typically 1 wt%, as determined by sending part of the sample to Galbraith Laboratories for chemical analysis.

Based on previous studies of metal carbonyl decomposition on oxide supports (e.g., Al_2O_3 and SiO_2) (*19, 20*) it was suggested that pretreatment of the support could be an important variable in the catalyst preparation procedure. In addition, the as-received titania may contain organic contaminants which should be removed prior to the deposition of highly dispersed iron. Thus, a series of "standard pretreatments" were given to titania before it was exposed to $Fe(CO)_5$. These are summarized in Table 1. Each sample was cleaned using the first pretreatment sequence in this table, which is similar to that described by Munuera *et al.* (*21*). The effectiveness of this pretreatment sequence was tested by heating the titania to 600 K in vacuum (10^{-2} Pa). The cleaned material remained white while the powder which was not cleaned turned blue-black during this evacuation. The color change following low temperature outgassing was attributed by Gebhardt and Herrington (*22*) to the diffusion of carbon impurities to the surface or to the reduction of titania by these impurities. After cleaning, the surface properties of titania (e.g., presence of hydroxyl groups, Ti^{3+}) were controlled using one of the three subsequent pretreatment sequences shown in the lower part of Table 1.

TABLE 1

Pretreatments of Titania

Purpose of pretreatment sequence	Environment	Time (h)	Temperature (K)
To clean titania	Oxygen	5	700
	Vacuum[a]	2	600
	Boiling water	0.15	380
	Air	16	380
Control surface properties, Sequence I	Vacuum[a]	4	600
Control surface properties, Sequence II	Vacuum[a]	5	720
Control surface properties, Sequence III	Vacuum[a]	2	720
	Oxygen	1	720
	Hydrogen	3	720
	Vacuum[a]	0.10	298

[a] 10^{-2} Pa.

Mössbauer spectroscopy. The Mössbauer spectrometer used in the present study has been described elsewhere (*17*). It was operated in the constant acceleration mode, with positive velocity corresponding to the source moving toward the absorber. All Mössbauer spectra were folded and fit by computer using the program MFIT (*23*). The Doppler velocity scale was calibrated with $Na_2Fe(CN)_5NO$ and a metallic iron foil. Isomer shifts are reported relative to metallic iron at room temperature.

Two *in situ* Mössbauer spectroscopy cells were used: one to study the decomposition of $Fe(CO)_5$ on titania and another to monitor the chemical state of iron after reduction in hydrogen at high temperatures (e.g., 800 K). The first cell was constructed of stainless steel and it allowed *in situ* Mössbauer spectra to be collected at temperatures from 77 to 700 K and at pressures from atmospheric to ca. 10^{-4} Pa. This cell has been described by Phillips *et al.* (*17*).

The second cell was composed of a quartz and a stainless-steel section, the latter section containing two Mylar windows for γ-ray transmission through the cell. The sample could be slid to the quartz section of the cell where high-temperature pretreatments could be performed, and it could then be slid to the stainless-steel section of the cell where room temperature Mössbauer spectra could be collected. This cell operated at pressures from atmospheric to ca. 10^{-4} Pa, and its construction has been described by Santos (*18*).

Samples for Mössbauer spectroscopy were in the form of circular pellets 2.3 cm in diameter. These pellets were fabricated from 0.4 g of titania by pressing the powder between two sheets of grafoil (sheets of graphite crystallites from Union Carbide) at a pressure of 1000–2000 psi. One sheet of grafoil was subsequently removed from the pellet, and the pellet was loaded into one of the Mössbauer spectroscopy cells. The sample was pretreated (as described previously), cooled to room temperature, and then dosed with a known quantity of $Fe(CO)_5$ by means of the glass transfer-bulb containing gaseous iron carbonyl. The cell was subsequently heated to 370–380 K to decompose the iron carbonyl on titania. The presence of the grafoil supporting sheet did not significantly affect the decomposition reaction, since the Mössbauer spectrum characteristic of $Fe(CO)_5$ decomposed on grafoil (17) was not observed in the present study.

Ammonia synthesis kinetics. For ammonia synthesis studies, a stoichiometric $H_2:N_2$ gas mixture was passed through a quartz, tubular reactor at a total pressure of ca. 0.1 MPa. The gaseous ammonia concentration in the reactor effluent was determined by simultaneous scrubbing and colorimetric titration. Accordingly, the gaseous effluent was bubbled through a standardized acid indicator solution made from sulfuric acid, distilled and deionized water, and bromophenol blue indicator. The details of this method of ammonia determination and a description of the ammonia synthesis reactor system have been presented elsewhere (24).

The amount of the catalyst used in the kinetic studies was chosen such that no more than 30% of the equilibrium conversion was reached. Due to the low activity of most of the catalysts studied, the reactor was normally operated at even lower conversions. Volumetric flowrates were varied from 1.2 to 3.3 $cm^3\ s^{-1}$ (at NTP) during synthesis. Different partial pressures of ammonia were obtained when the flowrate of the synthesis gas was changed, and the relation between the overall ammonia synthesis rate and the partial pressure of ammonia was thereby studied at temperatures between ca. 650 and 700 K. After reaction kinetics studies, the catalyst was cooled to room temperature and the synthesis gas was switched to flowing helium, which was not purified. After about 0.5 h the catalyst was exposed to air. The catalyst was removed from the reactor, and CO chemisorption, X-ray diffraction, and/or Mössbauer spectroscopy were used to characterize the catalyst.

Carbon monoxide chemisorption. Carbon monoxide chemisorption was used to determine the dispersion of metallic iron for the various Fe/TiO_2 samples. Adsorption studies on pure titania (pretreated and reduced in the same manner as Fe/TiO_2) showed that ca. 0.80 μmol of CO is adsorbed irreversibly at 300 K per gram of TiO_2. Previous work has assumed that each CO molecule chemisorbed titrates two iron atoms on the surface (*25*), and this ratio of CO to Fe was used in the present study. The CO chemisorption studies were performed using the constant volume, glass vacuum system mentioned in the section on catalyst preparation. The CO gas (Matheson minimum purity 99.99%) was purified by passing it through hot copper turnings (at ca. 500 K) and then through 13× molecular sieves immersed in a dry ice–acetone bath (193 K). The N_2 and He used in adsorption studies (for BET measurements

and for determining dead-volumes, respectively) were purified in a similar manner, with the exception that the 13× molecular sieves were kept at 77 K.

Prior to CO chemisorption measurements, each Fe/TiO_2 sample was reduced in hydrogen at 673 K, evacuated for 1 h at 673 K, and then cooled to 193 K (dry ice–acetone temperature). A first adsorption isotherm was generated by successively dosing known amounts of CO into a Vycor cell containing the sample. The catalyst was then evacuated for 1 h at room temperature and a second isotherm was collected at 193 K. The extent of irreversible CO adsorption reported in the present study is the difference between the two isotherms at a pressure of 13.3 kPa. This pressure chosen for the subtraction of the two isotherms has been used by other investigators (*1, 26*). For each CO chemisorption performed, a total surface area determination (BET) was also performed using the adsorption of nitrogen at 77 K. This was done assuming a cross-section for each N_2 molecule of 0.162 nm^2.

X-ray diffraction. X-ray line broadening was used to estimate the metallic iron particle size for those Fe/TiO_2 catalysts which contained metallic iron particles larger than ca. 5 nm. A Picker biplanar diffractometer with a scintillation counter and with 1° slits before and after the sample was used. X-ray diffraction patterns were obtained with Ni-filtered copper radiation. The samples were exposed to air during the collection of the X-ray diffraction patterns. An average crystallite size was calculated from the breadth of the (110) peak of α-Fe using the Scherrer equation. The peak width was corrected for instrumental broadening and the $K\alpha_1\alpha_2$ doublet, as described by Klug and Alexander (*27*). The former correction was made by measuring under similar conditions the line widths of a standard sample (i.e., Al) composed of large (>100 nm) particles.

RESULTS

Characterization of Fe/TiO_2 Catalysts

Table 2 presents the range of metallic iron particle sizes (from X-ray line broadening) and CO chemisorption uptakes for Fe/TiO_2 samples prepared by different methods. The samples prepared by incipient wetness impregnation using aqueous solution were characterized following reduction

TABLE 2

Characterization of Fe/TiO_2 Catalysts

Method of catalyst preparation	Iron loading (wt%)	Metallic iron particle size[a] (nm)	CO uptake (μmol g^{-1})	Percentage of iron in metallic state	Metallic iron dispersion[b] (%)
Thermal decomposition of iron pentacarbonyl	1.14	—	34.58	95.6	35.36
Nonaqueous impregnation	5	100	13.98	96.8	3.20
Incipient wetness impregnation with aqueous solution	5	65	—	87.6	—
Incipient wetness impregnation with acid solution	5	46	25.00	89.8	6.21
Fe/SiO_2; incipient wetness impregnation	15	—	10.23	82.0	0.93

[a] From X-ray line broadening using the (110) diffraction peak.

[b] From CO chemisorption, assuming a surface stoichiometry CO/Fe = ½.

in hydrogen at 670 K and exposure to air at room temperature. The samples prepared by nonaqueous impregnation and the thermal decomposition of $Fe(CO)_5$ were characterized after use of these samples as catalysts for ammonia synthesis.

Figure 1 shows room temperature Mössbauer spectra for three of the Fe/TiO_2 samples listed in Table 2: (a) prepared by incipient wetness impregnation using acid solution, (b) prepared by nonaqueous impregnation, and (c) prepared by thermal decomposition of $Fe(CO)_5$. The Mössbauer spectrum of a silica-supported sample containing 15 wt% Fe, prepared by incipient wetness impregnation, is also shown in this figure. All of the above samples were first studied as ammonia synthesis catalysts and then exposed to air for collection of the Mössbauer spectra. The six-peak pattern in each of these spectra is due to metallic iron. Computer fits of these spectra, the results of which are shown by the solid curves through the data points, indicated that the Mössbauer parameters of each of these sextuplets were essentially identical to those of bulk metallic iron. Furthermore, these spectra show that metallic iron is, in fact, the predominant form of iron in these samples. The small peak near zero velocity is due to the negative-most peak of a quadrupole-split doublet due to Fe^{3+} (the positive-most peak of this doublet overlaps with peak 4 of the metallic iron sextuplet, numbering these six peaks from negative to positive velocities). The presence of Fe^{3+} is undoubtedly the result of exposing these samples to air during collection of the Mössbauer spectra.

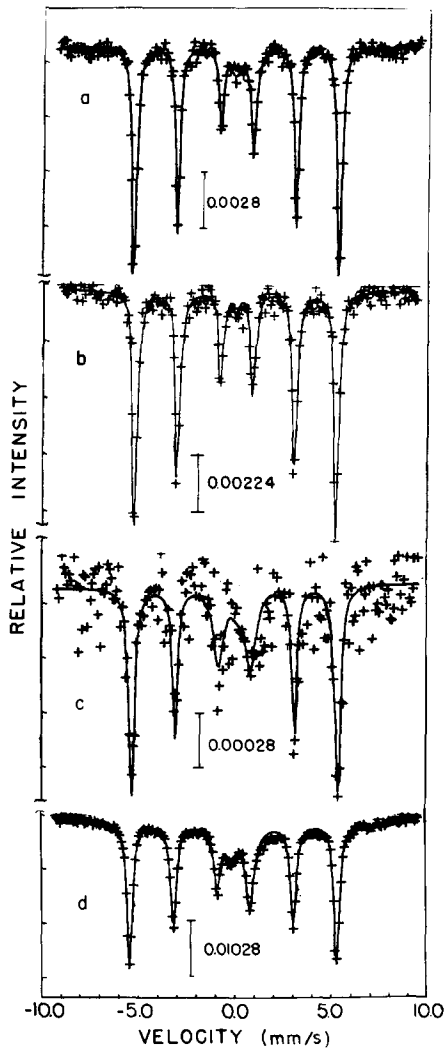

FIG. 1. Room temperature Mössbauer spectra of reduced Fe/TiO_2 and Fe/SiO_2 catalysts: (a) 5% Fe/TiO_2 prepared by incipient wetness impregnation using acid solution, (b) 5% Fe/TiO_2 prepared by nonaqueous impregnation, (c) 1.14% Fe/TiO_2 prepared by $Fe(CO)_5$ decomposition, (d) 15% Fe/SiO_2 prepared by incipient wetness impregnation. Samples exposed to air during collection of Mössbauer spectra, and vertical bars indicate the transmission scale of each spectrum.

Assuming that the recoil-free fractions for metallic iron and Fe^{3+} are equal, it is possible to estimate from the Mössbauer spectra the fraction of the iron in the metallic state for the samples of Fig. 1. The result of such spectral area calculations are summarized in Table 2. Accordingly, more than about 85% of the iron in all samples is metallic. Knowing this metallic fraction and the CO adsorption uptake, the metallic iron dispersion (or percentage exposed) was calculated for each sample, assuming that one adsorbed CO molecule titrates two surface iron atoms. Table 2 also shows these values.

According to Table 2, thermal decomposition of iron pentacarbonyl on titania in a

static system was the best method used in this study to prepare small metallic iron particles supported on TiO_2. Among the other three solution-based catalyst preparation methods, incipient wetness impregnation using an acid solution appears to be the best. This result is consistent with the idea that the basic nature of the support plays an important role in determining the dispersion of iron, as proposed by Murrell and Yates (*28*) for the preparation of supported Ru catalysts. Accordingly, hydrolysis of the OH groups on the support results in the precipitation of iron before it can be adsorbed on the support. Addition of acid to the solution suppresses the precipitation of iron, resulting in a higher dispersion of iron. The failure of nonaqueous impregnation to produce small iron particles, compared to the success of Murrell and Yates for Ru, could be due to the 0.5 wt% water content of the acetone used in the present study. It should be noted that the loading of iron in the samples made from incipient wetness impregnation and nonaqueous impregnation was about 5 wt% while the iron loading in the catalyst prepared from the thermal decomposition of iron carbonyl was close to 1 wt%. Differences in iron particle sizes obtained using these catalyst preparation procedures may be partially due to differences in iron loading.

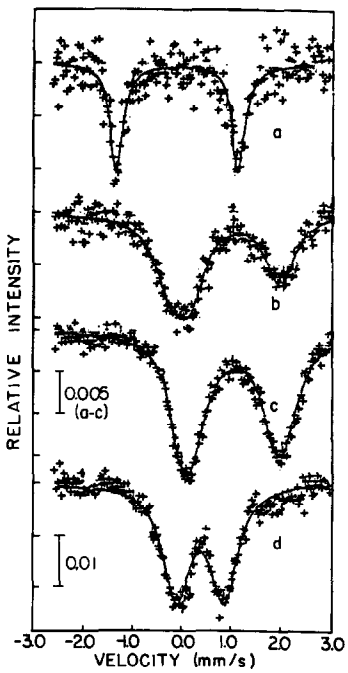

FIG. 2. Mössbauer spectra of $Fe(CO)_5/TiO_2$ after various treatments: (a) spectrum at 77 K after exposure of TiO_2 to $Fe(CO)_5$ at 298 K, (b) spectrum at 298 K after sample (a) had been heated to 380 K, (c) spectrum at 298 K after sample (b) had been heated to 673 K, (d) spectrum at 298 K after sample (c) had been exposed to air at 298 K. Vertical bars indicate the transmission scale of each spectrum.

Mössbauer Spectroscopy Studies of Fe/TiO_2 Samples Prepared via $Fe(CO)_5$ Decomposition

With the result that thermal decomposition of $Fe(CO)_5$ on titania could be used to prepare highly dispersed iron, *in situ* Mössbauer spectroscopy was used to study in greater detail the preparation and reduction of such samples. Consider first the decomposition of $Fe(CO)_5$ on TiO_2. Representative Mössbauer spectra are presented in Fig. 2. These are for a sample of TiO_2 which was pretreated in vacuum at 600 K (pretreatment sequence I in Table 1). Spectrum 2a was recorded at liquid nitrogen temperature after $Fe(CO)_5$ had been admitted to the sample cell. This spectrum is characteristic of $Fe(CO)_5$ which is physically adsorbed or frozen on the TiO_2 surface. Spectrum 2b was recorded at room temperature after the sample had been heated to 380 K for 10 h. This spectrum consists of two components: a quadrupole-split doublet (peaks near zero and 2 mm/s) indicative of Fe^{2+} and a singlet (near zero velocity) characteristic of zero-valent iron. The Mössbauer parameters (i.e., isomer shift, quadrupole splitting, and spectral area) of these two components were determined by computer fitting, assuming that the pair of peaks forming the spectral doublet had the same width and intensity. These Mössbauer parameters are given in Table 3 (sample 1), where it can be seen that 66% of the spectral area of Fig. 2b is due to the Fe^{2+} doublet. Spectrum 2c was recorded at room temperature after the

TABLE 3

Computer-Fit Mössbauer Parameters for Spectra Obtained at Room Temperature following $Fe(CO)_5$ Decomposition on Titania Samples Subjected to Different Pretreatments

Sample number	Pretreatment[a]	Decomposition temperature (K)	Total[b] spectral area	Fe^{2+}			Fe^{0}	
				QS	IS	%	IS	%
1	Sequence I	380	0.58	1.8	1.04	66	−0.29	34
		673	1.00	1.8	1.04	96	−0.12	4
2	Sequence III	380	0.33	1.9	1.09	70	−0.28	30
		673	0.49	1.6	1.00	99		
3	Sequence II	380	0.23	1.6	1.02	59	−0.27	41
		673	0.30	1.9	1.04	96	−0.15	4
4	Sequence II	380	0.33	1.7	1.06	58	−0.33	42
		723	0.55	1.7	1.05	96	−0.12	4
5	Sequence III	380	0.22	2.0	1.00	89	−0.24	11

[a] Sequences of pretreatment described in Table I.
[b] Normalized to sample #1 after high-temperature (673 K) decomposition.

sample had been subsequently heated to 673 K in vacuum. This spectrum is almost entirely that of an Fe^{2+} species. Table 3 indicates that 96% of the spectral area is due to this species. Spectrum 2d was recorded at room temperature after the sample had been exposed to air at this temperature. This is the spectrum of an Fe^{3+} species, showing that exposure to oxygen fully oxidized all of the iron on titania. Finally, Table 3 presents the results of computer fitting of analogous Mössbauer spectra collected for four other samples (two samples given pretreatment sequence II and two samples given pretreatment sequence III, as defined in Table 1).

The effects of various reduction treatments on the Mössbauer spectrum of a Fe/TiO_2 sample prepared by the thermal decomposition of $Fe(CO)_5$ are shown in Fig. 3. The titania was first subjected to pretreatment sequence III in Table 1, followed by $Fe(CO)_5$ decomposition at 380 K and hydrogen treatment at 673 K for 16 h. The resulting sample contained 1.38 wt% Fe, as shown by subsequent chemical analysis. The sample was then exposed to air at room temperature, pressed into pellet form, and transferred to the previously described Mössbauer spectroscopy cell (composed of quartz and stainless-steel sections). This was followed by rereduction in synthesis gas for ca. 16 h at 673 K with the sample in the glass section of the cell. During this time, the temperature was raised to 713 K for 1 h. The sample was cooled to room temperature, slid to the metal section of the cell, and a Mössbauer spectrum was collected (Fig. 3a). This procedure was then repeated after treatment in $H_2:N_2$ for 16 h at 673 K and 1 h at 773 K, and after subsequent treatment for 16 h at 673 K and 1 h at 798 K. The corresponding room temperature Mössbauer spectra are shown in Figs. 3b and c, respectively. Hydrogen was passed through the cell at room temperature during collection of these spectra. The sample was next exposed to air at room temperature for 3 h, transferred to a glass cell, and rereduced at 673 K prior to CO chemisorption measurements. The extent of irreversible CO adsorption was determined (31.3 μmol/g) and the sample was loaded into the Mössbauer spectroscopy cell where it was rereduced at 673 K for 21 h and at 693 K for 3 h. A room temperature Mössbauer spectrum was collected (Fig. 3d). For comparison, Fig. 3e shows the Mössbauer spectrum of a metallic iron foil. Noteworthy is the fact that the total area of

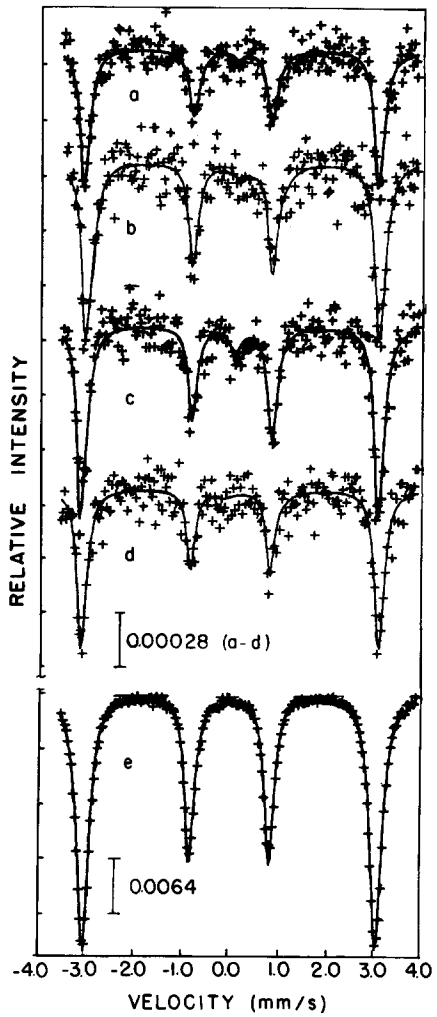

FIG. 3. *In situ* Mössbauer spectra at room temperature of 1.38 Fe/TiO_2 prepared by $Fe(CO)_5$ decomposition and reduced at progressively higher temperatures: (a) reduced at 713 K, (b) reduced at 773 K, (c) reduced at 798 K, (d) exposed to air at 298 K and reduced at 693 K, (e) metallic iron foil. Vertical bars indicate the transmission scale of each spectrum.

each spectrum in Fig. 3 cannot be compared with the others. This is due to the loss of powder from the pellet during its transfer between the glass and metal sections of the Mössbauer spectroscopy cell, and also to the fact that a new pellet with a smaller amount of sample was used after exposure to air and re-reduction at 693 K.

Table 4 summarizes the results of computer fitting the spectra of Figure 3. Three doublets were used to fit these spectra and the intensities of widths of the pair of peaks comprising each doublet were constrained to be equal. The quadrupole splittings (QS) and isomer shifts (IS) of these doublets were obtained from the computer-fit peak positions. The two doublets with the larger quadrupole splitting (i.e., the four outer peaks) are peaks of the six-peak Mössbauer spectrum due to metallic iron. (The other two peaks of the six-peak spectrum are located at positions outside the velocity interval scanned.) The doublet with the smallest quadrupole splitting is due to an iron species different from metallic iron. The percentage of the total spectral area due to this central doublet is determined by the equation

$$\% \text{ central doublet} = 100\, A_D/[2(A_2 + A_3 + A_4 + A_5) + A_D]$$

where A_D is the area of the central doublet and $2(A_2 + A_3 + A_4 + A_5)$ is the area of the six metallic iron peaks. (The relative areas of the six peaks of metallic iron are $A_1 : A_2 : A_3 : A_4 : A_5 : A_6 = 3 : 2 : 1 : 1 : 2 : 3$. Thus, the total area of the six peaks is equal to two times the area of the four inner peaks.) Table 4 also gives the magnetic hyperfine field of metallic iron, H, calculated from the splitting of the two outermost peaks of the spectra in Fig. 3. It should be mentioned that the Mössbauer spectra of Fig. 3 can also be represented adequately by replacing the central doublet with a spectral singlet located near zero velocity. This has no effect on the observed trend that the spectral area of this component increases when the reduction temperature is increased to 798 K, and it decreases following exposure to air at room temperature and reduction at 693 K. However, the calculated isomer shift of this component is dependent on whether a spectral doublet or a singlet is used in the computer fitting. Thus, the reported values of isomer shift and quadrupole splitting for the central doublet reported in Table 4 can be taken to have only qualitative validity.

TABLE 4

Mössbauer Parameters for 1.38 wt% Fe/TiO_2 Prepared by Thermal Decomposition of $Fe(CO)_5$ and Reduced at Progressively Higher Temperatures

Reduction temperature (K)	Relative spectral area of central doublet (%)	Central doublet		Four outer peaks				H (kOe)
		QS (mm/s)	IS (mm/s)	QS (mm/s)	IS (mm/s)	QS (mm/s)	IS (mm/s)	
713	1.4	0.703	0.438	1.655	−0.009	6.161	−0.017	330.4
773	1.5	0.449	0.372	1.695	−0.032	6.165	−0.013	330.7
798	4.6	0.737	0.410	1.685	−0.002	6.180	−0.027	331.6
693[a]	2.7	1.203	0.445	1.658	−0.012	6.193	0.004	332.2
Iron foil	—	—	—	1.691	−0.018	6.166	−0.018	330.7

[a] Reduction after exposure to air at room temperature.

Ammonia Synthesis Kinetics

For the purpose of the present study the measured overall rate of ammonia production, r, is expressed in a power-law form,

$$r = \frac{k}{P_{NH_3}{}^m}$$

where P_{NH_3} is the ammonia partial pressure in the reactor effluent, m is the negative reaction order with respect to ammonia pressure, and k is an apparent rate constant which incorporates the temperature dependence of the rate for a fixed ammonia pressure and feed composition (i.e., stoichiometric $H_2 : N_2$ mixture). In general, the apparent activation energy, E_A, has two contributions: one from the activation energy for nitrogen chemisorption and the other from the heat of ammonia adsorption (e.g., 29). The reaction order, m, is, in general, a function of the partial pressure of ammonia.

Three Fe/TiO_2 samples were studied as catalysts for ammonia synthesis. These were prepared by (i) incipient wetness impregnation using an acid solution, (ii) nonaqueous impregnation, and (iii) $Fe(CO)_5$ decomposition. Prior to collection of ammonia synthesis kinetics, each catalyst was reduced in synthesis gas at ca. 675 K for about 1 week until a constant catalytic activity was observed. During that time, catalysts (i) and (iii) were also treated for 1 h at 713 K. Figure 4 is a log–log plot of r versus P_{NH_3} at different temperatures (below 700 K) for the Fe/TiO_2 sample prepared by incipient wetness impregnation using an acid solution. After these data were collected, the sample was heated to 798 K for 1 h, and the ammonia synthesis data of Fig. 5 were obtained. The catalyst was then exposed to air at room temperature for several days, followed by rereduction in synthesis gas at 675 K for several days and 713 K for 1 h. The ammonia synthesis kinetics subsequently measured are shown in Fig. 6. The temperature dependence of the ammonia synthesis rate at a constant ammonia pressure of 5 Pa is shown in Fig. 7. It can be seen therein that the apparent activation energy (from the slope of these plots) increases when the maximum reduction tem-

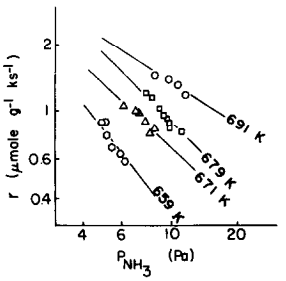

FIG. 4. Dependence of the ammonia synthesis rate, r, on the ammonia partial pressure for 5% Fe/TiO_2 prepared by incipient wetness impregnation using acid solution and reduced at 713 K.

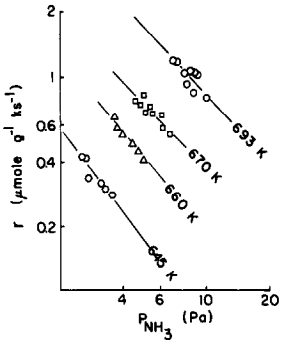

FIG. 5. Dependence of the ammonia synthesis rate, r, on the ammonia partial pressure for 5% Fe/TiO_2 of Fig. 4 followed by reduction at 798 K.

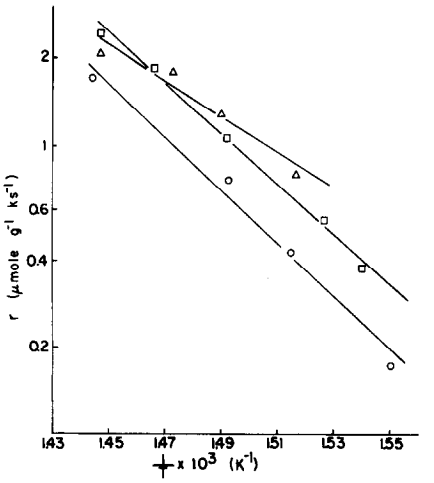

FIG. 7. Arrhenius plots at P_{NH_3} = 5 Pa for 5% Fe/TiO_2 prepared by incipient wetness impregnation using acid solution and (△) reduced at 713 K, (○) followed by reduction at 798 K, (□) followed by exposure to air at 298 K and reduction at 713 K.

perature is increased from 713 to 798 K, and it subsequently is decreased slightly upon exposure to air at room temperature followed by rereduction at 713 K. The results of similar studies of the Fe/TiO_2 sample prepared by nonaqueous impregnation are shown in Figs. 8–10. In particular, Figure 8 shows the ammonia synthesis kinetics measured after reduction at 675 K, Figure 9 shows the reaction kinetics obtained after the catalyst was subsequently heated to 773 K for 44 h, and Figure 10 shows the temperature dependence of the ammonia synthesis rate at a constant ammonia pressure of 5 Pa.

Table 5 summarizes values of the apparent activation energy, E_A, and the negative reaction order (with respect to ammonia pressure), m, for the above two catalysts after different reduction temperatures. Values of the ammonia synthesis apparent turnover frequency N at 673 K and an ammonia pressure of 5 Pa were also calculated by appropriate extrapolation of the reaction kinetics data and combination with the results of CO chemisorption. Also included in Table 5 is a summary of the results of ammonia synthesis studies on a Fe/TiO_2 catalyst prepared by $Fe(CO)_5$ decomposition, following 1 h reductions at 713, 773, and 798 K. (Plots of ln r versus ln P_{NH_3} for this catalyst have been reported elsewhere

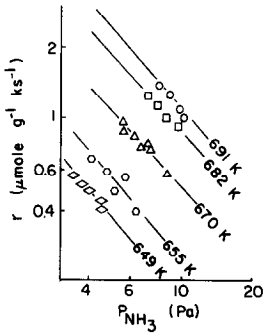

FIG. 6. Dependence of the ammonia synthesis rate, r, on the ammonia partial pressure for 5% Fe/TiO_2 of Fig. 5 followed by exposure to air at room temperature and reduction at 713 K.

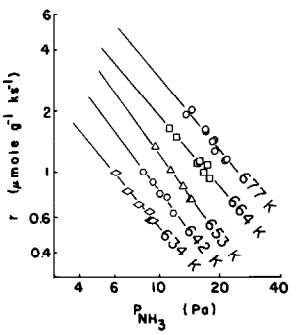

FIG. 8. Dependence of the ammonia synthesis rate, r, on the ammonia partial pressure for 5% Fe/TiO_2 prepared by nonaqueous impregnation and reduced at 677 K.

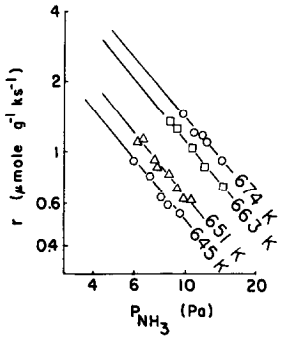

FIG. 9. Dependence of the ammonia synthesis rate, r, on the ammonia partial pressure for 5% Fe/TiO_2 of Fig. 8 followed by reduction at 773 K.

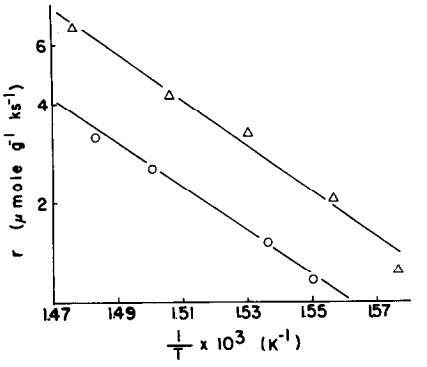

FIG. 10. Arrhenius plots at P_{NH_3} = 5 Pa for 5% Fe/TiO_2 prepared by nonaqueous impregnation and (△) reduced at 677 K, (○) followed by reduction at 773 K.

(*30*).) Finally for comparison, values of E_A, m, and N are also included in Table 5 which are typical of small metallic iron particles (ca. 2–5 nm in size) supported on MgO (*31*) and of large metallic iron particles (greater than ca. 10 nm in size) on SiO_2 (*18*) and MgO (*31*).

DISCUSSION

Interactions of Titania with Iron Species Formed via Decomposition of Fe(CO)$_5$

The Mössbauer spectra of Fig. 2 show that the decomposition of $Fe(CO)_5$ on titania at 380 K leads primarily to the forma-

TABLE 5

Kinetic Parameters for Ammonia Synthesis at 101 kPa

Catalyst	Reduction temperature (K)	E_A Apparent activation energy[a] (kJ mol^{-1})	N Apparent turnover frequency[b] (ks^{-1})	m Reaction order with respect to ammonia partial pressure[c]
1.14% Fe/TiO_2; $Fe(CO)_5$ decomposition	713	100	0.031	0.44
	773	190	0.016	0.62
	798	220	0.011	0.77
5% Fe/TiO_2; nonaqueous impregnation	677	135 (127)	0.48	1.26
	773[d]	127 (122)	0.23	1.20
5% Fe/TiO_2; incipient wetness (acid solution)	713	117	0.036	0.97
	798	177	0.016	1.14
	713[e]	164	0.021	1.13
15% Fe/SiO_2	673	90	149	0.40
1% Fe/MgO	673	100	10	0.50
40% Fe/MgO	673	73	70	0.50

[a] At P_{NH_3} = 5 Pa (values in parentheses at 10 Pa).
[b] At ca. 673 K, P_{NH_3} = 5 Pa.
[c] Defined by equation $m = -\partial(\ln r)/\partial(\ln P_{NH_3})$.
[d] Reduced at this temperature for 44 h.
[e] Exposed to air at room temperature for 3 days prior to reduction.

tion of highly dispersed Fe^{2+}. This behavior is apparently independent of the pretreatments given to titania, as shown by Table 3. To interpret these results, a brief description of the surface properties of titania is given below. In air, the surface of TiO_2 is largely covered by water and hydroxyl groups. A number of investigators have studied how the surface concentrations of these species vary with sample treatment (*21, 32–40*). In short, most of the water is removed from the surface by evacuation at temperatures up to ca. 650 K, while a significant surface coverage by hydroxyl groups (e.g., 1 OH/nm^2) may remain after outgassing at ca. 650 K. Dehydroxylation of the surface is accompanied by the formation of coordinatively unsaturated Ti^{4+} cations. Vacuum treatment of titania at temperatures higher than ca. 770 K or hydrogen treatment at temperatures higher than ca. 670 K may lead to the removal of surface oxygen, accompanied by the reduction of Ti^{4+} to Ti^{3+}. The discoloration of titania which goes from a light gray, following outgassing at 670 K, to blue, following outgassing above 773 K or hydrogen reduction at above 670 K, is caused by the presence of reduced titanium cations. This reduction process has been studied using electron spin resonance (*41–44*).

Based on the above discussion, it is possible to speculate about the state of the titania surface following each of the three sample treatments described in Table 1. Following Treatment I (evacuation at 600 K) the surface may contain a significant number of hydroxyl groups and some surface water may also be present. The surface does not, however, have an appreciable amount of Ti^{3+}. The color of titania was white. Following Treatment II (evacuation at 720 K) the surface concentration of hydroxyl groups is expected to be lower than that after Treatment I, and the surface is probably free of water. In addition, Ti^{3+} cations may be present in the sample. The color of titania was gray. The surface coverage of titania by hydroxyl groups after Treatment III (evacuation, oxidation in O_2, and reduction in H_2 at 720 K) may be similar to that after Treatment II. In contrast, the sample may contain an appreciable number of Ti^{3+} cations. The color of the sample was blue.

The result that the Mössbauer spectra were essentially the same after $Fe(CO)_5$ decomposition on titania samples having received Treatments I, II, and III indicates that Ti^{3+} cations do not apparently participate in the decomposition process to a significant extent. (In fact, recent X-ray photoelectron spectroscopy studies (*45, 46*) have shown that the Ti^{3+} cations formed during the reduction of TiO_2 at ca. 800 K are located primarily in the bulk.) The common feature of all three titania surfaces is the presence of hydroxyl groups. Thus, the decomposition of $Fe(CO)_5$ on titania to give primarily Fe^{2+} must be related to the presence of hydroxyl groups on the surface of titania. Consistent with this conclusion is the observation in Table 3 that the Mössbauer spectral area after $Fe(CO)_5$ decomposition on a titania sample given Treatment I is significantly greater than the spectral area of samples given Treatments II or III. Since titania subjected to Treatment I is expected to have a higher surface concentration of hydroxyl groups (and possibly surface water) than samples subjected to Treatments II and III, it is suggested that hydroxyl groups serve as binding sites for the adsorption of iron carbonyl or other iron species (e.g., subcarbonyl species) formed as intermediates during the decomposition of $Fe(CO)_5$. This statement is in agreement with previous studies (*19, 20 47, 48*) of $Mo(CO)_6$ decomposition on γ-Al_2O_3. Specifically, the amount of Mo deposited on the alumina surface was observed to decrease as the sample was pretreated to decrease the surface hydroxyl concentration. Finally, the fact that Fe^{2+} is the primary product of $Fe(CO)_5$ decomposition on titania is readily explained in terms of the aforementioned interaction of iron species with surface hydroxyl groups. As

discussed in the literature (e.g., see Refs. *19, 20, 48, 49*), hydroxyl groups may react with surface-bound metal carbonyl species to give dihydrogen and oxidized metal species. Indeed, the reaction of $Fe(CO)_5$ with hydroxyl groups on γ-Al_2O_3 has been shown to give Fe^{2+}, as observed in the present study of titania.

Besides Fe^{2+}, the Mössbauer spectra collected after $Fe(CO)_5$ decomposition on titania at 380 K show a spectral singlet near zero velocity (ca. -0.2 mm s^{-1}) which is characteristic of zero-valent iron. This iron species may be a metal subcarbonyl bound to a surface hydroxyl group. For example, Brenner and Hucul (*50*) used temperature-programmed methods to study the interaction of $Fe(CO)_5$ with γ-Al_2O_3. Dihydrogen was evolved by $Fe(CO)_5/Al_2O_3$ over a wide range of temperatures (from ca. 370 to 900 K), leading these authors to conclude that Fe^{2+} and iron subcarbonyl species were present on the surface and that the conversion of iron subcarbonyl species to Fe^{2+} became more complete as the temperature was increased. This is exactly the behavior observed in Table 3 of the present paper, where it can be seen that the Mössbauer spectral area of the zero-valent iron decreases (and the spectral area of Fe^{2+} increases) when the sample is heated from 380 to 670 K. Finally, it should be noted that the present study of $Fe(CO)_5$ decomposition on titania is also consistent with the work of Hagnes *et al.* (*51*) who found that the decomposition of $Fe_3(CO)_{12}$ on MgO at 393 K led to the production of both Fe^{2+} and a zero-valent iron species (identified as superparamagnetic metallic iron).

Evidence for Metal–Support Interactions between Metallic Iron and Titania

Samples prepared by iron carbonyl decomposition. As discussed above, thermal decomposition of $Fe(CO)_5$ on titania leads to the formation of highly dispersed Fe^{2+} and zero-valent iron species. After prolonged treatment in hydrogen at ca. 700 K, the Mössbauer spectroscopy results of Fig. 3 and Table 4 indicate that a large fraction of this Fe^{2+} is reduced to the metallic state. Moreover, the Mössbauer parameters of the metallic iron particles on titania are essentially identical to those of bulk metallic iron. The results of Table 2 also indicate that these particles chemisorb a significant amount of carbon monoxide. It is thus concluded that "normal" metallic iron (i.e., α-Fe) is formed upon treatment of Fe/TiO_2 samples in hydrogen at 700 K. This is in agreement with the work of Tatarchuk and Dumesic (*10, 14–16*) who used electron microscopy, Mössbauer spectroscopy, and X-ray photoelectron spectroscopy to study iron supported on thin films of TiO_2.

The ammonia synthesis kinetic parameters E_A and m (see Table 5) observed on the Fe/TiO_2 sample prepared by $Fe(CO)_5$ decomposition and reduced at 713 K are similar to those parameters reported for metallic iron particles supported on MgO (*31*) or SiO_2 (*18*). This is additional evidence that the iron particles on TiO_2 after reduction at 713 K behave as "normal" particles of metallic iron. It should be noted that the apparent turnover frequency for ammonia synthesis over Fe/TiO_2 after reduction at 713 K is significantly lower than the value for small metallic iron particles supported on MgO, and both of these values are lower than for large particles of metallic iron on MgO or SiO_2. This may be due to the fact that ammonia synthesis over iron is a structure-sensitive reaction, and it is difficult to compare apparent turnover frequencies for metallic iron particles of different size and/or shape. The particularly low turnover frequency over Fe/TiO_2 catalysts will be discussed in greater detail later in this paper.

When the Fe/TiO_2 catalyst prepared by $Fe(CO)_5$ decomposition is reduced at 773 and then at 798 K, the apparent activation energy and reaction order with respect to ammonia pressure are observed to be significantly greater than those values for metallic iron supported on MgO or SiO_2. One of the slow steps in ammonia synthesis over

iron is the activated chemisorption of nitrogen and this process is accompanied by electron transfer from iron to nitrogen (*29*). The increase in apparent activation energy may therefore suggest that titania-supported iron becomes electron deficient upon increasing the reduction temperature above ca. 770 K. This would also explain the increase in the reaction order with respect to ammonia pressure for increasing reduction temperatures, since the strength of ammonia adsorption would be expected to increase as electrons are transferred from iron to titania, as discussed elsewhere (*30*). Regardless of the proposed direction of electron transfer between iron and titania, the ammonia synthesis results indicate that a metal–support interaction is initiated by reduction at temperatures near 770 K of Fe/TiO_2 samples prepared by $Fe(CO)_5$ decomposition. In results presented elsewhere (*30*) it has also been shown that the extent of CO chemisorption on a Fe/TiO_2 catalyst prepared by $Fe(CO)_5$ decomposition decreases by an order of magnitude when the reduction temperature is increased from 713 to 798 K, while the BET surface area remains unchanged.

While the above results of ammonia synthesis and CO chemisorption show that a metal–support interaction between iron and titania exists after hydrogen treatment at temperatures near 770 K, the Mössbauer spectra of Fig. 3 show that the electronic properties of metallic iron are not altered when the reduction temperature is increased from 713 K to either 773 or 798 K. The only observable change in the Mössbauer spectrum is the growth of the paramagnetic component (i.e., central doublet), comprising 1.4 and 4.6% of the total spectral area after reduction at 713 and 798 K, respectively. Any description of the nature of the metal–support interaction between iron and titania must therefore rationalize the observation that a bulk technique, like Mössbauer spectroscopy, is not particularly sensitive to the metal–support interaction while surface probes, like ammonia synthesis kinetics and CO chemisorption, are changed dramatically when the interaction is initiated by reduction at ca. 770 K. One such description is that the interaction between iron and titania is restricted to the surface of the metallic iron particles, with the interior of the iron particles remaining unperturbed by titania as discussed later in this paper.

It is interesting to speculate that the paramagnetic component in the Mössbauer spectrum may be related to iron atoms which are interacting with titania near the surface of the metallic iron particles. The increase in spectral area of this doublet upon increasing the reduction temperature from 713 to 798 K would suggest an increase in the number of iron atoms interacting with titania. Of significance is the observation that the spectral area of this paramagnetic component decreased from 4.6 to 2.7% of the total spectral area when the sample, after reduction at 798 K, was exposed to air at room temperature, followed by reduction at 693 K. This would suggest that the interaction between iron and titania which is initiated by hydrogen treatment at ca. 770 K can be at least partially destroyed by exposure to air at room temperature. In fact, this behavior is shown more clearly by the results of CO chemisorption reported elsewhere (*30*). Specifically, the extent of CO chemisorption on Fe/TiO_2 increases by an order of magnitude when a sample which has been reduced at 798 K is exposed to air at room temperature and reduced at 673 K. It should be noted that it has been well established that exposure to oxygen or water at elevated temperatures can destroy interactions of metals with titania (e.g., *1, 2*). In addition, Mériaudeau *et al.* (*7*) also reported that metal–support interactions on titania could be destroyed by exposure to air at room temperature.

Samples prepared by impregnation. As presented in the results section of this paper, the size of the metallic iron particles on titania prepared by impregnation methods

were much larger than the iron particles prepared by $Fe(CO)_5$ decomposition. The observed ammonia synthesis kinetics over these large particles of metallic iron suggest that these particles may show the same interactions with titania which were exhibited by the small particles prepared by $Fe(CO)_5$ decomposition. In particular, the Fe/TiO_2 sample prepared by incipient wetness impregnation using an acid solution contained metallic iron particles ca. 20 nm in diameter, and the ammonia synthesis kinetic parameters, E_A and m, were observed to increase significantly when the reduction temperature was raised from 713 to 798 K. In addition, the interaction between these large metallic iron particles and titania, initiated by hydrogen treatment at 798 K, appears to be partially destroyed by exposure to oxygen at room temperature followed by reduction at 713 K. This is evidenced by a small, but measurable, decrease in E_A (see Table 5).

It is noteworthy that the ammonia synthesis turnover frequency following reduction at 713 K of the Fe/TiO_2 catalyst prepared by incipient wetness impregnation using an acid solution is significantly lower than that expected for 20 nm metallic iron particles. From the results of Tatarchuk and Dumesic (*10, 14–16*) it can be suggested that 20-nm metallic iron particles on titania should be three-dimensional crystallites (i.e., not thin pillboxes) after hydrogen treatment at ca. 700 K. The lower turnover frequency over these iron particles supported on titania indicates, therefore, that the surfaces of these crystallites are different from the surfaces of "normal" α-Fe crystallites of the same size. This is further evidence that an interaction between iron and titania takes place at the surface of the metallic iron particles. If this interaction took place only at the surface of contact between the metal crystallite and the titania support, then three-dimensional crystallites as large as 20 nm would have a significant number of surface atoms which were not interacting with titania. These metal crystallites would be expected to have ammonia synthesis turnover frequencies similar to those values for iron particles on SiO_2 or MgO, contrary to the observations of Table 5. Therefore, the low turnover frequency over the 20 nm iron crystallites on titania suggests that the entire surface of the metallic iron particles may interact with titanium species, i.e., titanium species may be present on the surface of the metallic iron particles. The possible modes of transport of titanium species from the support to the surface of metallic iron particles will be discussed later in this paper.

The Fe/TiO_2 sample prepared by nonaqueous impregnation contains very large metallic iron particles (ca. 30 to 100 nm as viewed by CO chemisorption and X-ray diffraction, respectively). The ammonia synthesis kinetic parameters, E_A and m, are not sensitive to changes in the reduction temperature from 677 to 773 K. In addition, the ammonia synthesis turnover frequency over this catalyst is significantly higher than that over the Fe/TiO_2 catalysts prepared by $Fe(CO)_5$ decomposition or incipient wetness impregnation using an acid solution. Compared to these latter two catalysts, the interaction between iron and titania is apparently not as extensive on the sample prepared by nonaqueous impregnation.

Nature of Metal–Support Interactions between Metallic Iron and Titania (52)

In short, it can be suggested from the above discussion that a metal–support interaction between iron and titania exists at the surface of metallic iron particles. This interaction is due to the presence of titanium species on the surface of the metallic iron particles since the interior of the particles is unaffected by the metal–support interaction. This simple model explains all of the observations of the present study. After reduction at temperatures lower than ca. 700 K, these titanium species merely block iron ensembles for ammonia synthesis. The values of E_A and m for the remaining surface iron ensembles are characteristic of

those values for "normal" metallic iron. Since an iron ensemble containing an appreciable number of surface iron atoms (e.g., 7) is believed to be required for ammonia synthesis (*53*), a small number of titanium species can decrease dramatically the number of active sites for ammonia synthesis while the extent of CO chemisorption would be hardly diminished. This explains the low ammonia synthesis turnover frequencies, the "normal" values of the ammonia synthesis kinetic parameters E_A and m, and the appreciable extents of CO chemisorption for Fe/TiO_2 catalysts reduced at temperatures near 700 K. Upon reduction at temperatures higher than ca. 770 K, a larger fraction of the iron surface may become covered by titanium species, as discussed below. In addition, the titanium species may be reduced below the tetravalent state (e.g., *10, 42, 43*). Electron transfer between the surface iron atoms and these reduced titanium species could then take place, thereby changing the values of E_A and m and suppressing the extent of CO chemisorption at room temperature. Since the above interactions take place at the surface of the iron particles, a bulk technique such as Mössbauer spectroscopy is insensitive to the interactions and large particles of metallic iron can demonstrate such metal–support interactions. It is important to note that the presence of titanium species on the surface of Pt particles supported on TiO_2 has also been suggested by Mériaudeau *et al.* (*54*). A detailed description of the possible consequences of these surface titanium species has been proposed elsewhere (*55*).

If the above model is, in fact, correct one must explain the mode by which titanium species are transported from the titania support to the surface of the metallic iron particles. More than one mode probably exists. Consider first Fe/TiO_2 samples prepared by impregnation methods. In order to prevent precipitation of iron hydroxides during incipient wetness impregnation using aqueous solution, it was necessary to use acid solutions. At low pH, however, the dissolution of titania in water is favored (e.g., $TiO(OH)_2 \rightarrow TiO(OH)^+ + OH^-$). For example, the pH of a saturated aqueous solution of ferric nitrate (i.e., iron concentration of 0.88 mol/liter) is about 0.2. The concentration of $TiO(OH)^+$ in this solution can be estimated to be about 3.15×10^{-3} mol/liter (*56*). Accordingly, the Ti/Fe molar ratio in solution would be 0.0036. If all of this titanium remains associated with the surface of iron particles formed during subsequent catalyst treatments and if the dispersion of these metallic iron particles is 5% (a value typical of 20 nm particles), then the Ti/Fe atomic ratio at the surface of the metallic iron particles would be 0.07. Thus, one mode of titanium transport to the surface of metallic iron particles may be the dissolution of titanium species during impregnation using aqueous solutions. Indeed, the Fe/TiO_2 catalyst prepared by nonaqueous impregnation did not show significant interactions between iron and titania.

The presence of titanium species at the surface of metallic iron particles prepared by $Fe(CO)_5$ decomposition indicates that another mode of titanium transport must exist. This mode may be the spreading of reduced titanium species on the surface of metallic iron. For example, consider the following argument. Group VIII metal particles (e.g., Pt) have been observed to spread (forming thin pillboxes) over reduced titania surfaces in hydrogen at temperatures near 770 K (*4*). The energy required to convert 1 mol of bulk Pt to a (111) monolayer of Pt is about 65 kcal. This energy is presumably compensated by the energy gained in forming the metal–support interaction between Pt and reduced titania. Is it possible, however, that reduced titanium species may also spread over Group VIII metals to take advantage of metal–support interactions? First, the mobility of these species would have to be comparable to that of a Group VIII metal. Mobility is often related to the melting point of the material, and indeed, the melting and boiling

points of TiO and Pt are essentially identical (*56*). Second, it may be thought that the ionic bonding in bulk TiO (rock salt structure) would preclude the formation of a TiO monolayer, due to the long range nature of electrostatic forces. However, even if the bonding in TiO were completely ionic, the energy required to convert 1 mol of bulk TiO to a (100) monolayer of TiO would be about 70 kcal. (This calculation utilizes the known Madelung constants for bulk TiO and for a (100) surface having the rock salt structure (*57*).) Thus, it may be concluded that the energetics of reduced titanium species (e.g., TiO) spreading over Group VIII metals are similar to those of Group VIII metals spreading over reduced titania. This may be another mode by which titanium species can be transported to the surface of metallic iron.

For small metallic iron particles, as prepared by $Fe(CO)_5$ decomposition, the above transport process may lead to the presence of a small amount of titanium species over the surface of the entire particle after treatment in hydrogen at elevated temperatures. For larger iron particles, as prepared by nonaqueous impregnation, the spreading rate of these species over iron may be such that only a fraction of the iron surface may contain titanium species. This would explain why these particles did not show significant metal–support interactions.

Once reduced titanium species are present on the surface of metallic iron following reduction at elevated temperatures (e.g., 770 K) one must explain how exposure to air at room temperature, followed by reduction at 700 K, restores the "normal" surface properties of metallic iron. First, any electron transfer between reduced titanium species and surface iron atoms which is initiated by high temperature reduction will be destroyed when the surface titanium species and surface iron atoms are oxidized at room temperature. Accordingly, the properties of normal metallic iron would be achieved by hydrogen treatment at 700 K, at which temperature the iron, but not the oxidized titanium species, would be rereduced. In addition, the heat which is generated when the reduced titanium species are oxidized to TiO_2 may be sufficient to give these species the mobility required to nucleate into three-dimensional TiO_2 islands on the iron surface. In short, it is possible that titanium species may be sufficiently mobile to spread over and interact strongly with the iron surface in hydrogen during high temperature reduction and then to form three-dimensional islands of TiO_2 on the iron surface during subsequent exposure to oxygen at room temperature. Upon rereduction at high temperatures, reduced titanium species could again spread over the iron surface.

CONCLUSIONS

Impregnation methods using aqueous and nonaqueous solutions were found to be unsuccessful for the preparation of small metallic iron particles (e.g., less than 10 nm in size) supported on titania. However, the use of iron carbonyl decomposition at 380 K followed by hydrogen treatment at 700 K led to metallic iron particles with dispersions as high as ca. 35%. During the decomposition process at 380 K, the iron carbonyl interacts with hydroxyl groups (and possibly water) on the titania surface, forming Fe^{2+} and subcarbonyl species on the support; and, during hydrogen treatment at 700 K these species are reduced to metallic iron.

Metal–support interactions are initiated when the reduction temperature of the Fe/TiO_2 catalysts is increased from 700 to ca. 770 K. These interactions are manifested by changes in the kinetics of ammonia synthesis and by a suppression of CO chemisorption. Such phenomena can be observed for iron particles as large as 20 nm. In addition, Mössbauer spectra of the iron particles show "normal" metallic iron (i.e., α-Fe) after reduction at 700 and 770 K. Hence, the metal–support interaction is re-

stricted to the surface of the metallic iron particles.

There may be several modes by which titanium species are transported from the support to the surface of the metallic iron particles: this may occur in aqueous solution during catalyst preparation or it may be due to the spreading of reduced titanium species (e.g., TiO) over the surface of iron during reduction at high temperatures. The interaction between iron and titania can be partially destroyed by exposure of Fe/TiO_2 to air at room temperature, during which the titanium species and iron atoms near the metallic iron surface are undoubtedly oxidized to Ti^{4+} and Fe^{3+}, respectively. The heat liberated during this process may provide sufficient mobility to the titanium species to allow the nucleation of three-dimensional TiO_2 islands on the surfaces of the iron particles. During subsequent reduction at high temperatures, the reduced titanium species may once again spread over the metallic iron surface.

CONCLUDING REMARKS

The results of the present study are indicative of a "strong metal-supported interaction" between iron and titania. It has also been shown that metallic iron particles are not merely on the surface of the titania support and therefore only interacting through the geometric area of contact between the metal and support. Instead, titanium species are also present on the surface of the metallic iron particles. This behavior may explain a number of observations reported in the literature regarding interactions of titania with Group VIII metals. For example, the possible presence of titanium species on the surface of Pt particles supported on titania has been suggested by Mériaudeau *et al.* (*54*), as mentioned earlier in this paper. In addition, Fung (*8*) has mentioned that large particles (ca. 10 nm) of Pt and Pd show suppressed hydrogen adsorption and absorption, respectively, when they are supported on titania; and, Turlier *et al.* (*58*) have reported the suppression of hydrogen adsorption on large particles of nickel (16 nm) supported on titania. It seems difficult to interpret these results on large metal particles without postulating the presence of titanium species on the surface of these particles. It should also be noted that one reaction for which titania-supported metals may be particularly active is Fischer–Tropsch synthesis. One explanation for this enhanced activity when the metal is supported on titania has been in terms of the formation of active sites at the interface between the metal particle and the titania support (*59, 60*). If titanium species are present on the surface of the metal particle, however, then these special sites may also be created over the entire surface of the metal particle and not only at the geometric area of contact between the metal particle and the support. This could explain why large particles of Ni (5–8 nm) show methanation activities which are significantly greater than Ni on silica or alumina, and also why these particles are resistant to the formation of $Ni(CO)_4$ in the presence of gaseous CO (*6*). Finally, it should not be implied from the above remarks that all strong metal–support interactions reported in the literature (and denoted by SMSI) for Group VIII metals supported on titania are due necessarily to the presence of titanium species on the surfaces of the metal particles. Instead, it is suggested that the acronym "SMSI" is an umbrella under which a number of different phenomena may be covered. Some of these phenomena may possibly involve electron transfer through the geometric area of contact between a small metal particle and the support on which it is bonded while others may not.

ACKNOWLEDGMENTS

We gratefully acknowledge the graduate and professional opportunities program at the University of Wisconsin which provided a fellowship to J.S. We also thank Kodak for the funding which supported J.P. during this work, and we acknowledge financial support from the National Science Foundation during the latter stages of this work. We are indebted to C. Naccache

(Institut de Recherches sur la Catalyse), R. Madon (Exxon), and R. T. K. Baker (Exxon) for their insightful comments during the preparation of this manuscript.

REFERENCES

1. Tauster, S. J., Fung, S. C., and Garten, R. L., *J. Amer. Chem. Soc.* **100,** 170 (1978).
2. Tauster, S. J., and Fung, S. C., *J. Catal.* **55,** 29 (1978).
3. Baker, R. T. K., Prestridge, E. B., and Garten, R. L., *J. Catal.* **56,** 390 (1979).
4. Baker, R. T. K., Prestridge, E. B., and Garten, R. L., *J. Catal.* **59,** 293 (1979).
5. Tauster, S. J., Fung, S. C., Baker, R. T. K., and Horsley, J. A., *Science* **211,** 1121 (1981).
6. Vannice, M. A., and Garten, R. L., *J. Catal.* **56,** 236 (1979).
7. Mériaudeau, P., Ellestand, O. H., Dufaux, M., and Naccache, C., *J. Catal.* **75,** 243 (1982).
8. Fung, S. C., *J. Catal.* **76,** 225 (1982).
9. Kao, C. C., Tsai, S. C., Bahl, M. K., Chung, Y. M., and Lo, W. L., *Surface Sci.* **95,** 1 (1980).
10. Tatarchuk, B. J., and Dumesic, J. A., *J. Catal.* **70,** 323 (1981).
11. Bahl, M. K., Tsai, S. C., and Chung, Y. W., *Phys. Rev. B* **21,** 1344 (1980).
12. Horsley, J. A., *J. Amer. Chem. Soc.* **101,** 2870 (1979).
13. Imelik, B., Naccache, C., Coudurier, G., Praliaud, H., Mériaudeau, P., Gallezot, P., Martin, G. A., and Vedrine, J. C. (Eds.), *Stud. Surf. Sci. Catal.* **11,** 1982.
14. Tatarchuk, B. J., and Dumesic, J. A., *J. Catal.* **70,** 308 (1981).
15. Tatarchuk, B. J., and Dumesic, J. A., *J. Catal.* **70,** 335 (1981).
16. Tatarchuk, B. J., Chludzinski, J. J., Sherwood, R. D., Dumesic, J. A., and Baker, R. T. K., *J. Catal.* **70,** 433 (1980).
17. Phillips, J., Clausen, B., and Dumesic, J. A., *J. Phys. Chem.* **84,** 1814 (1980).
18. Santos, J., M.S. Thesis, University of Wisconsin (1982).
19. Brenner, A., and Burwell, R. L., Jr., *J. Catal.* **52,** 364 (1978).
20. Brenner, A., and Burwell, R. L., Jr., *J. Catal.* **52,** 353 (1978).
21. Munuera, G., Moreno, F., and Gonzalez, F., *in* "Seventh Int. Sym. on the Reactivity of Solids," (J. S. Anderson, M. W. Roberts, and F. S. Stone, Eds.), p. 681. Chapman & Hall, London, 1972.
22. Gebhardt, J., and Herrington, K., *J. Phys. Chem.* **62,** 120 (1958).
23. Sørensen, K., in "LTE. II. Internal Report No. 1, 1972." Laboratory of Applied Physics II, Technical University of Denmark, Lyngby.
24. Holzman, P. R., Shiflett, W. K., and Dumesic, J. A., *J. Catal.* **62,** 167 (1980).
25. Boudart, M., Delbouille, A., Dumesic, J. A., Khammouma, S., and Topsøe, H., *J. Catal.* **37,** 486 (1975).
26. Sinfelt, J. H., and Yates, J. C., *J. Catal.* **8,** 82 (1967).
27. Klug, H. P., and Alexander, L. E., "X-ray Diffraction Procedure," 2nd ed. Wiley, New York, 1974.
28. Murrell, L. L., and Yates, D. J. C., "Scientific Bases for Preparation of Heterogeneous Catalysts," Second International Symp., Belgium, C-1, 1978.
29. Ozaki, A., and Aika, K., *in* "Catalysis: Science and Technology" (J. R. Anderson, and M. Boudart, Eds.), Vol. I, pp. 87–158. Springer-Verlag, New York, 1981.
30. Santos, J., and Dumesic, J. A., *Stud. Surf. Sci. Catal.* **11,** 43 (1982).
31. Dumesic, J. A., Topsøe, H., Khammouma, S., and Boudart, M., *J. Catal.* **37,** 503 (1975).
32. Boehm, H. P., *Adv. Catal.* **16,** 179 (1969).
33. Primet, M., Pichat, P., and Mathieu, M. V., *C.R. Acad. Sci. Paris B* **267,** 799 (1968).
34. Iyengar, R. D., and Codell, M., *Adv. Colloid Interface Sci.* **3,** 365 (1972).
35. Jackson, P., and Parfitt, G. D., *Trans. Faraday Soc.* **67,** 2469 (1971).
36. Munuera, G., and Stone, F. S., *Disc. Faraday Soc.* **52,** 205 (1971).
37. Kiselev, A. V., and Uvarov, A. V., *Surf. Sci.* **6,** 399 (1967).
38. Primet, M., Basset, J., Mathieu, M. V., and Prettre, M., *J. Phys. Chem.* **74,** 2868 (1970).
39. Kaluza, U., and Boehm, H. P., *J. Catal.* **22,** 347 (1971).
40. Lake, I. J. S., and Kemball, C., *Trans. Faraday Soc.* **63,** 2535 (1967).
41. Cornaz, P. F., Van Hoof, J. H. C., Pluijm, F. J., and Schuit, G. C. A., *Disc. Faraday Soc.* **41,** 290 (1966).
42. Gravelle, P. L., Juillet, F., Mériaudeau, P., and Teichner, G. J., *Disc. Faraday Soc.* **52,** 140 (1971).
43. Iyengar, R. D., Codell, M., Karra, J. S., and Turkevich, J., *J. Amer. Chem. Soc.* **88,** 5055 (1966).
44. Mashchenko, A. I., Kazanskii, V. B., Pariskii, G. B., and Sharapov, V. N., *Kinet. Katal.* **8,** 853 (1967).
45. Sexton, B. A., Hughes, A. E., and Foger, K., *J. Catal.* **77,** 85 (1982).
46. Chien, S. H., Shelimov, B. N., Resasco, D. E., Lee, E. H., and Haller, G. L., *J. Catal.* **77,** 301 (1982).
47. Burwell, R. L., Jr., and Brenner, A., *in* "Catalysis, Heterogeneous and Homogeneous" (B.

Delmon and G. Jannes, Eds.), p. 157. Elsevier, Amsterdam, 1975.

48. Bowman, R. G., and Burwell, R. L., Jr., *J. Catal.* **63,** 463 (1980).

49. Brenner, A., Hucul, D. A., and Hardwick, S. J., *Inorg. Chem.* **18,** 1478 (1979).

50. Brenner, A., and Hucul, D. A., *Inorg. Chem.* **18,** 2836 (1979).

51. Hagnes, F., Bussiere, P., Basset, J. M., Courmereuc, D., Chauvin, Y., Bonnevoit, L., and Oliver, D., *in* "Proc. of the 7th Int. Cong. on Catal., Tokyo 1980" (T. Seiyama, and K. Tanabe, Eds.), p. 418. Elsevier, Amsterdam, 1981.

52. Some of the ideas contained in this section were developed during discussions with C. Naccache.

53. Dumesic, J. A., Topsøe, H., and Boudart, M., *J. Catal.* **37,** 513 (1975).

54. Mériaudeau, P., Dutel, J. F., Dufaux, M., and Naccache, C., *Stud. Surf. Sci. Catal.* **11,** 95 (1982).

55. Jiang, X. Z., Hayden, T., and Dumesic, J. A., *J. Catal.*, submitted.

56. "Lange's Handbook of Chemistry" (J. A. Dean, Ed.), 12th ed., pp. 5–12, McGraw–Hill, New York, 1979.

57. Piela, L., and Andzelm, J., *Surf. Sci.* **84,** 179 (1979).

58. Turlier, P., Dalmon, J. A., and Martin, G. A., *Stud. Surf. Sci. Catal.* **11,** 203 (1982).

59. Burch, R., and Flambard, A. R., *JCS Chem. Commun.* 123 (1981).

60. Burch, R., and Flambard, A. R., *Stud. Surf. Sci. Catal.* **11,** 193 (1982).